Topological Dynamical Decoupling with Complete Pulse Error Cancellation

Nayden P. Nedev[1] and Nikolay V. Vitanov[1]
[1] *Center for Quantum Technologies, Department of Physics, Sofia University, 5 James Bourchier Boulevard, 1164 Sofia, Bulgaria*
(Dated: October 21, 2025)

Systematic pulse errors remain a major obstacle to high-fidelity quantum control. We present a new family of dynamical decoupling sequences, denoted Tn, that achieve exact cancellation of pulse area errors to all orders by enforcing a simple topological phase condition. Unlike some conventional composite sequences, Tn requires no numerical optimization and admits closed-form analytic phases for arbitrary sequence length, while providing substantial robustness to detuning as well. We demonstrate these sequences on superconducting transmon qubits from both IBM Quantum processor ibm_torino and IQM Quantum processor Garnet, observing population plateaus in close agreement with theory. These results establish a new paradigm for hardware-efficient error suppression, broadly applicable across quantum computing, sensing, and memory platforms.

Dynamical decoupling (DD) is a cornerstone technique for mitigating decoherence in quantum systems, offering a practical and hardware-efficient means of prolonging coherence without the overhead of full quantum error correction [1–8]. Its utility has been repeatedly demonstrated on noisy intermediate-scale quantum devices (NISQ), where experimental constraints preclude large-scale fault-tolerant schemes [9–15]. The essence of the method lies in the application of carefully timed and phased control pulses to average unwanted environmental interactions, thus suppressing errors due to both dephasing and relaxation processes.

Although traditional DD protocols, such as CPMG [16, 17], UDD [18], KDD [19], and XY-based sequences [20–22], compensate for errors up to a given order in system–environment couplings, their accuracy remains inherently finite, especially in the presence of systematic control imperfections such as pulse area errors. Dynamical decoupling techniques used to combat dephasing in NMR are known in the literature as rephasing [23]. Such composite pulse methods from NMR have shown that phase engineering can mitigate these errors, but typically only in a finite error range. Here, we present an exact analytic construction of topological dynamical decoupling sequences with infinite order suppression of systematic pulse area errors, while simultaneously achieving significant robustness to detuning errors too.

This class of sequences, denoted Tn, is derived from a simple criterion imposed on the phases, and is demonstrated on superconducting transmon qubits using IBM's ibm_torino and IQM's Garnet processors. By "topological", we mean that the cancellation of errors is not achieved by delicate fine-tuning, but is enforced by a global constraint on the control phases. Unlike conventional DD, where robustness is finite-order and depends on perturbative expansions, here this topological condition ensures complete error cancellation, independent of microscopic details.

The dynamics of a qubit due to an external pulsed interaction is described by a propagator U, which is conveniently parameterized with the complex Cayley-Klein parameters a and b as

$$U = \begin{bmatrix} a & b \\ -b^* & a^* \end{bmatrix}. \tag{1}$$

For exact resonance ($\Delta = 0$), the Schrödinger equation is solved exactly for any $\Omega(t)$. Then the Cayley-Klein parameters depend only on the pulse area $A = \int_{t_i}^{t_f} \Omega(t) dt$,

$$a = \cos(A/2), \quad b = -i \sin(A/2), \tag{2}$$

with $\Omega(t)$ assumed real. The transition probability is $p = |b|^2 = \sin^2(A/2)$, and hence, complete population inversion occurs for $A = \pi$ (π pulses) or odd-integer multiples of π. This inversion is sensitive to variations in the pulse area: a small deviation from the value π, i.e., $A = \pi(1 + \xi)$, causes an error in the inversion of order $\mathcal{O}(\xi^2)$,

$$p = 1 - \pi^2\xi^2/4 + \mathcal{O}(\xi^4). \tag{3}$$

A constant phase shift ϕ in the Rabi frequency, $\Omega(t) \to \Omega(t)e^{i\phi}$, is imprinted into the propagator (1) as

$$U(A, \phi) = \begin{bmatrix} a & be^{i\phi} \\ -b^* e^{-i\phi} & a^* \end{bmatrix}. \tag{4}$$

A sequence of N pulses, each with area A_k and phase ϕ_k, produces the propagator

$$U^{(N)} = U_{\phi_N}(A_N) U_{\phi_{N-1}}(A_{N-1}) \cdots U_{\phi_1}(A_1). \tag{5}$$

The objective of any rephasing sequence is to produce the identity propagator,

$$\mathbf{I} = \begin{bmatrix} 1 & 0 \\ 0 & 1 \end{bmatrix}, \tag{6}$$

as closely as possible, i.e., by compensating deviations in the relevant parameters to the highest possible order. We define the rephasing error ϵ as the distance between the actual propagator $\mathbf{U}$ and the target propagator $\mathbf{I}$:

$$\epsilon = |U_{11} - 1| + |U_{12}|. \tag{7}$$

The propagator (4) can be written in the form

$$U(A,\phi) = e^{-\frac{iA}{2}M(\phi)}, \tag{8}$$

where

$$M(\phi) = \begin{bmatrix} 0 & e^{i\phi} \\ e^{-i\phi} & 0 \end{bmatrix}, \tag{9}$$

and $A = \pi(1+\xi)$.

The objective of the present work is to find a set of phases ϕ_k for which all systematic errors in the pulse area are compensated. This leaves us with the sequence of the form (10) that we require to be equal to the identity for any deviation ξ from an ideal π pulse. The deviation ξ is consistent for all pulses,

$$U^{(n)} = \prod_{k=1}^{n} e^{-i\frac{A}{2}M(\phi_k)} = I \tag{10}$$

To fulfill Eq. (10), we need to impose two conditions on the phases ϕ_k and $M(\phi_k)$ matrices, respectively,

1. All pairs of neighboring $M(\phi_j), M(\phi_k)$ matrices need to commute.
2. The phases must be chosen such that $\sum_{k=1}^{n} M(\phi_k) = 0$.

If the two conditions are fulfilled, then

$$U^{(n)} = \exp\left(-i\frac{A}{2}\sum_{k=1}^{n} M(\varphi_k)\right) = I. \tag{11}$$

From condition 1 we find

$$[M(\phi_k), M(\phi_j)] = 2i\sin(\phi_k - \phi_j)\sigma_z, \tag{12}$$

where σ_z is the z Pauli matrix. This result shows us that any two matrices $M(\phi_j), M(\phi_k)$ commute if and only if $\sin(\phi_k - \phi_j) = 0$. Therefore, $\phi_k - \phi_j$ must be an integer multiple of π. Condition 2 requires

$$\sum_{k=1}^{n} M(\varphi_k) = \begin{bmatrix} 0 & \sum_{k=1}^{n} e^{i\varphi_k} \\ \sum_{k=1}^{n} e^{-i\varphi_k} & 0 \end{bmatrix} = 0 \tag{13}$$

Therefore, exact cancellation requires

$$\sum_{k=1}^{n} e^{i\varphi_k} = 0. \tag{14}$$

Now, suppose that the two consecutive phases are chosen such that condition one is fulfilled: $\phi_{k+1} = \phi_k \pm \pi$. Then, using the identity $e^{\pm(\phi\pm\pi)} = -e^{\pm\phi}$, their contributions to the exponential sum (14) are $e^{i\phi_k} + e^{i\phi_{k+1}} = e^{i\phi_k} + e^{i\phi_k+\pi} = e^{i\phi_k} - e^{i\phi_k} = 0$. Hence, each such pair cancels exactly. This leaves us with the following

$$|\phi_k - \phi_j| = \pi \quad (mod\ 2\pi) \tag{15}$$

Tn	Phases of Tn
T2	$(0, 1)\pi$
T4	$(0, 0, 1, 1)\pi$
T6	$(0, \frac{1}{3}, 0, 1, \frac{4}{3}, 1)\pi$
T8	$(0, \frac{1}{2}, \frac{1}{2}, 0, 1, \frac{3}{2}, \frac{3}{2}, 1)\pi$
T10	$(0, \frac{3}{5}, \frac{4}{5}, \frac{3}{5}, 0, 1, \frac{8}{5}, \frac{9}{5}, \frac{8}{5}, 1)\pi$
T12	$(0, \frac{2}{3}, 1, 1, \frac{2}{3}, 0, 1, \frac{5}{3}, 0, 0, \frac{5}{3}, 1)\pi$
T14	$(0, \frac{5}{7}, \frac{8}{7}, \frac{9}{7}, \frac{8}{7}, \frac{5}{7}, 0, 1, \frac{12}{7}, \frac{1}{7}, \frac{2}{7}, \frac{1}{7}, \frac{12}{7}, 1)\pi$
T16	$(0, \frac{3}{4}, \frac{5}{4}, \frac{3}{2}, \frac{3}{2}, \frac{5}{4}, \frac{3}{4}, 0, 1, \frac{7}{4}, \frac{1}{4}, \frac{1}{2}, \frac{1}{2}, \frac{1}{4}, \frac{7}{4}, 1)\pi$
T18	$(0, \frac{7}{9}, \frac{4}{3}, \frac{5}{3}, \frac{16}{9}, \frac{5}{3}, \frac{4}{3}, \frac{7}{9}, 0, 1, \frac{16}{9}, \frac{1}{3}, \frac{2}{3}, \frac{7}{9}, \frac{2}{3}, \frac{1}{3}, \frac{16}{9}, 1)\pi$
T20	$(0, \frac{4}{5}, \frac{7}{5}, \frac{9}{5}, 0, 0, \frac{9}{5}, \frac{7}{5}, \frac{4}{5}, 0, 1, \frac{9}{5}, \frac{2}{5}, \frac{4}{5}, 1, 1, \frac{4}{5}, \frac{2}{5}, \frac{9}{5}, 1)\pi$
T22	$(0, \frac{9}{11}, \frac{16}{11}, \frac{21}{11}, \frac{2}{11}, \frac{3}{11}, \frac{2}{11}, \frac{21}{11}, \frac{16}{11}, \frac{9}{11}, 0,$ $1, \frac{20}{11}, \frac{5}{11}, \frac{10}{11}, \frac{13}{11}, \frac{14}{11}, \frac{13}{11}, \frac{10}{11}, \frac{5}{11}, \frac{20}{11}, 1)\pi$
T24	$(0, \frac{5}{6}, \frac{3}{2}, 0, \frac{1}{3}, \frac{1}{2}, \frac{1}{2}, \frac{1}{3}, 0, \frac{3}{2}, \frac{5}{6}, 0,$ $1, \frac{11}{6}, \frac{1}{2}, 1, \frac{4}{3}, \frac{3}{2}, \frac{3}{2}, \frac{4}{3}, 1, \frac{1}{2}, \frac{11}{6}, 1)\pi$

TABLE I. Phases of several high-order Tn sequences.

as the only condition that we need to impose for any pair of neighboring pulses in the sequence to achieve compensation for any systematic error in pulse area. The presented derivation assumes that the system is in resonance ($\Delta = 0$). Still, we find that the results also hold for models where the Rabi frequency is an even function, while the detuning is an odd function of time, such as the Landau-Zener and Allen-Eberly models.

Using the newly derived condition, we present a new class of topological DD sequences which cancel exactly any systematic pulse area errors, while simultaneously providing substantial compensation in detuning Δ as shown in Fig.1. We start by fixing the sequence's structure to fulfill (15). Then, to determine the actual phases of the sequences, the elements of the resulting propagator $\boldsymbol{U}^{(n)}$ must satisfy the following conditions: $[\partial_\Delta^k U_{11}^{(n)}]_{\Delta=0} = 0$ and $[\partial_\Delta^k U_{12}^{(n)}]_{\Delta=0} = 0$, to the highest possible order. Here, we present the solution to the resulting system of algebraic equations that provides the greatest robustness to detuning.

Based on their structure, Tn sequences can be divided into two subclasses. The sequences T$4l$ of $4l$ pulses, where $l = 1, 2, ...$, have the structure

$$\mathrm{T}4l = (r_l)_0(r_l^{-1})_0(r_l)_\pi(r_l^{-1})_\pi, \tag{16}$$

where

$$(r_l)_0 = (\phi_1, \phi_2, \ldots, \phi_{l-1}, \phi_l) \tag{17a}$$

$$(r_l^{-1})_0 = (\phi_l, \phi_{l-1}, \ldots, \phi_2, \phi_1), \tag{17b}$$

$$(r_l)_\pi = (\phi_1+\pi, \phi_2+\pi, \ldots, \phi_{l-1}+\pi, \phi_l+\pi) \tag{17c}$$

$$(r_l^{-1})_\pi = (\phi_l+\pi, \phi_{l-1}+\pi, \ldots, \phi_2+\pi, \phi_1+\pi). \tag{17d}$$

The sequences T$2m$ of $2m$ pulses, where $m = 2j+1$ and $j = 0, 1, 2, ...$, have the structure

$$T2m = (r_m)_0(r_m)_\pi, \tag{18}$$

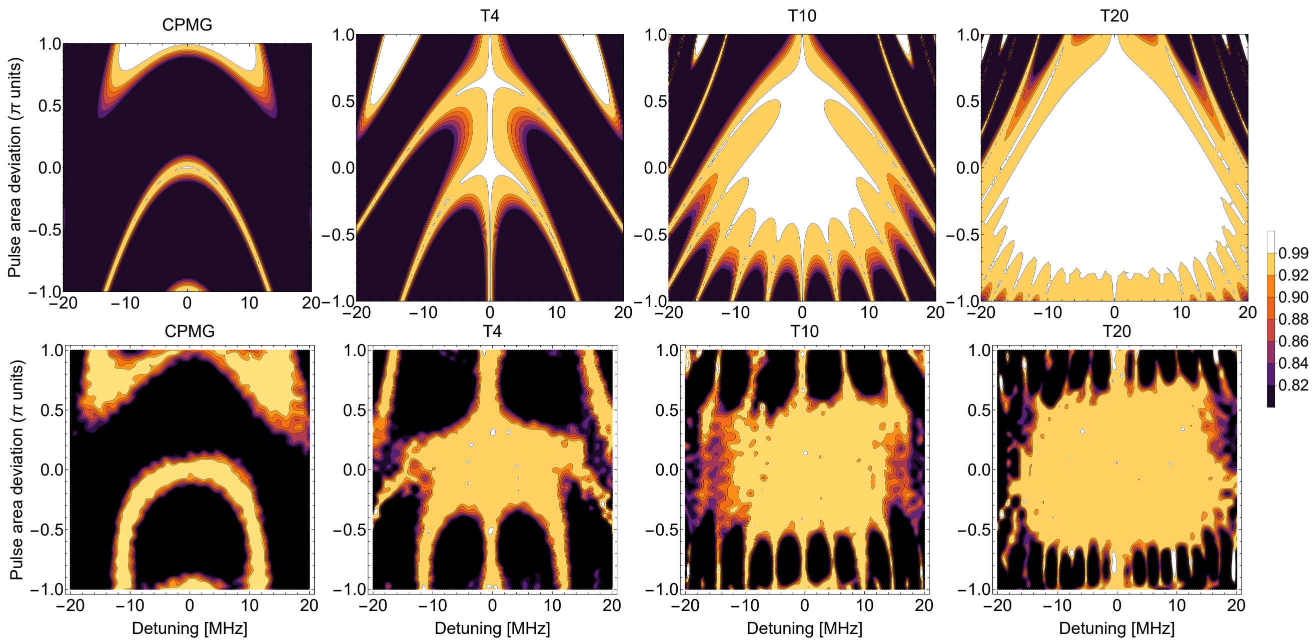

FIG. 1. Theoretical predictions (top) and measured results from IQM Garnet (bottom) of the $|0\rangle$-state population for several Tn sequences and CPMG with simultaneous deviations in both detuning and pulse area. The Rabi frequency is $\Omega = 2\pi \times 25$ MHz and the pulse duration is 20 ns.

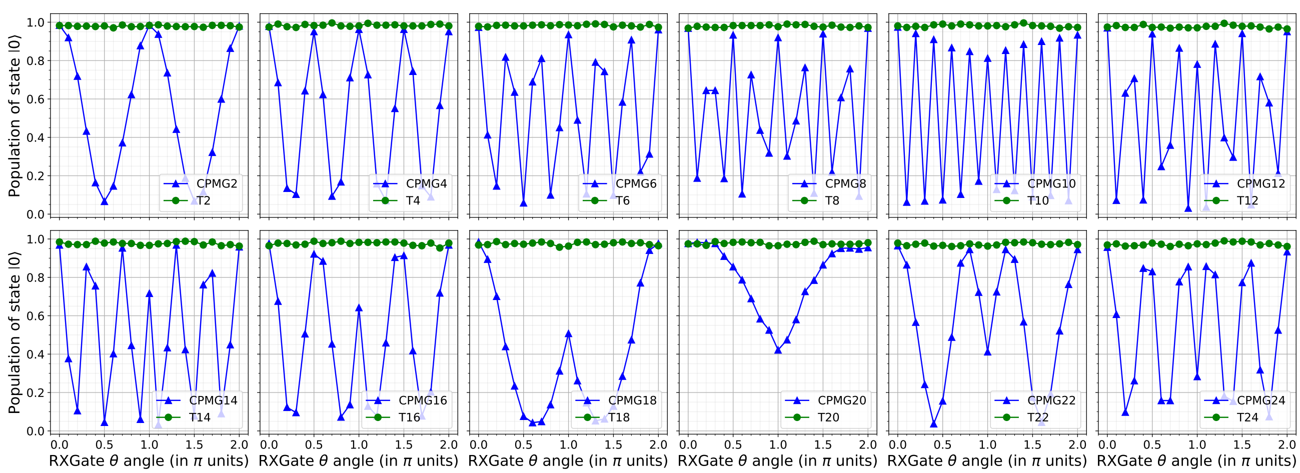

FIG. 2. Measured $|0\rangle$-state population for several Tn sequences on ibm_torino. Here, CPMGn denotes the sequence with the same number of pulses, but implemented without the phases for reference.

where

$$(r_m)_0 = (\phi_1, \phi_2, \ldots, \phi_{m-1}, \phi_m) \tag{19a}$$

$$(r_m)_\pi = (\phi_1 + \pi, \phi_2 + \pi, \ldots, \phi_{m-1} + \pi, \phi_m + \pi). \tag{19b}$$

The general formula for their phases is

$$\phi_k = \frac{(k-1)(n/2-k)}{n/2}\pi. \tag{20}$$

where n denotes the total number of pulses in the sequence and $k = 1, 2, \ldots, n$. The phases of the first few sequences of this class are listed in Table I.

We found that several of the URn sequences, introduced in [24], also satisfy condition (15). Therefore, UR4n (UR4, UR8, ...) also compensate any systematic pulse area errors.

In this work, we use qubit 10 of ibm_torino, one of IBM Quantum Heron r1 Processors. It is an open-access quantum processor that consists of 133 transmon qubits. The exact date of the demonstration was 05/08/2025. At the time of the demonstration, the parameters of the 10th qubit of the ibm_torino system were calibrated as follows: the coherence time T1 was 224 μs, the coherence time T2 was 256 μs, and the readout assignment

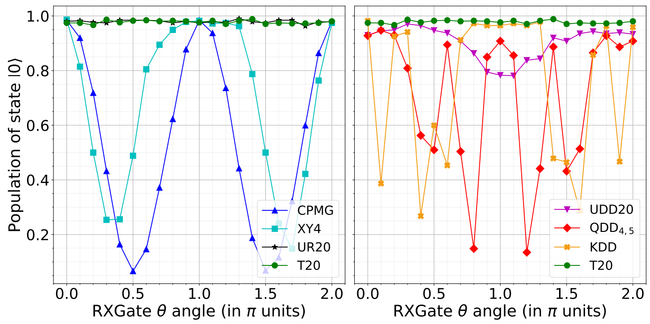

FIG. 3. Measured results on ibm_torino, comparing some of the most widely used types of DD sequences.

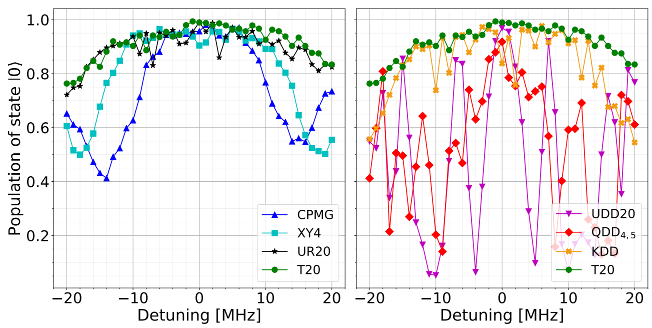

FIG. 4. Measured results on IQM Garnet, comparing some of the most widely used types of DD sequences.

error was 1.66%. The demonstrations were performed using $Rx(\theta)$ fractional gates [25], which allowed efficient implementation of $Rx(\theta)$ for an arbitrary rotation angle θ, avoiding the decomposition into multiple native gates. This allowed us to test an arbitrarily large deviation from an ideal π-pulse rotation (X gate) without relying on low-level control. Each $Rx(\theta)$ gate had a duration of 32 ns.

The demonstration consists of preparing the excited state $|1\rangle$ by applying an X gate to the ground state of the qubit $|0\rangle$. Then a DD sequence is applied by $Rx(\theta)$ with the corresponding phases added by $Rz(\phi)$ gates and symmetrical time delays between the pulses. The DD sequence is followed by another X gate and finally a measurement in the computational basis. Each circuit is repeated 512 times, and the results are averaged to obtain a single data point for our plots. Fig. 2 presents the measured results for the first Tn sequences, proving their robustness to any pulse area errors. In the next demonstration, Fig. 3 shows a comparison with the most widely used types of DD sequences. We observe that the performance of the newly introduced sequences, along with UR, remains unaffected by any pulse area deviations.

The other demonstrations are done using qubit 1 of IQM Garnet, a 20-qubit quantum processing unit based on superconducting transmon qubits. The demonstrations presented here are performed using the pulse-level access quantum computing module IQM Pulla [26]. The

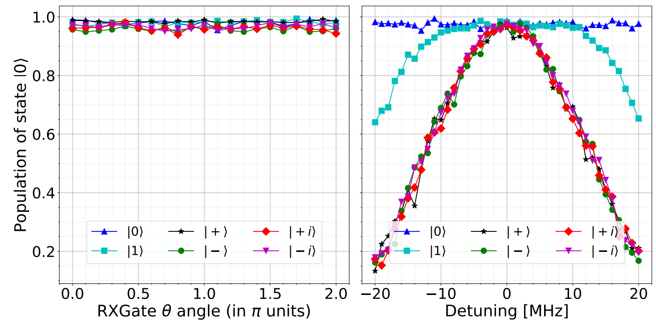

FIG. 5. Measured results on ibm_torino and IQM Garnet of T10 robustness for different initial states.

exact date of the demonstration was 06/09/2025. At the time of the demonstration, the parameters of the 1st qubit of the IQM Garnet system were calibrated as follows: the qubit frequency was 4.4955 GHz, the T1 coherence time was 44.45 μs, the T2 (Ramsey) coherence time was 5.88 μs, the T2 (echo) coherence time was 18.09 μs, and the readout assignment error was 2.10%. Here, we implemented the DD sequences using the native prx gates with their calibrated "drag_crf" implementation. Each pulse duration was 20 ns, and the pulse amplitude and drive frequency were varied. Again, each circuit was repeated 512 times, and the results were averaged to obtain a single data point for our plots. Figure 1 shows the measured results for simultaneous deviations in both pulse area and detuning using a 41 by 41 point grid for CPMG and several Tn sequences. The data demonstrate the scaling of the robust region with the order of the sequence. The deviations from the theoretical predictions are mostly due to SPAM errors that prevent achieving fidelities above 99%. In the following demonstration, Fig. 4 shows a comparison with the most widely used types of DD sequences against detuning. The data display superior performance to most DD sequences, with only URn showing comparable results. Fig. 5 illustrates that the complete pulse error compensation of Tn is independent of the initial state. However, the detuning robustness is worsened for the initial states $|+\rangle$, $|-\rangle$, $|+i\rangle$, and $|-i\rangle$. This demonstration follows the setup previously described; however, initially, the six Pauli eigenstates are prepared as $|\Psi\rangle = U|0\rangle$. Then a DD sequence is added, after that we apply $U^\dagger$, and finally measure in the computational basis.

We have introduced a new analytic family of dynamical decoupling sequences — Tn — that achieve exact cancellation of systematic pulse area errors to all orders, a property we term topological dynamical decoupling. The construction is rooted in a simple condition imposed on the pulse phases, leading to closed-form analytic expressions for an arbitrary order sequence. We demonstrate these sequences on a superconducting transmon qubits from both IBM Quantum processor ibm_torino and IQM Quantum processor Garnet, observing population plateaus in close agreement with theory. We also demonstrate superior performance to the most widely used types of DD sequences, with only UR showing comparable results, as expected from the theoretical predictions. These results open a new path for hardware-efficient quantum control, especially in architectures where systematic calibration drift is a limiting factor. We anticipate applications in quantum memories, quantum sensing, and error-protected gate synthesis, as well as integration into hybrid error mitigation and correction frameworks.

This research is supported by the Bulgarian Ministry of Education and Science under the National Program "Young Scientists and Postdoctoral Students – 2", by the Bulgarian national plan for recovery and resilience, Contract No. BG-RRP-2.004-0008-C01 (SUMMIT), Project No. 3.1.4, and by the European Union's Horizon Europe research and innovation program under Grant Agreement No. 101046968 (BRISQ). We acknowledge the use of the supercomputing cluster PhysOn at Sofia University for this work. We acknowledge the use of IBM Quantum services for this work. The views expressed are those of the authors and do not reflect the official policy or position of IBM or the IBM Quantum team. We acknowledge the use of IQM Resonance services for this work. The views expressed are those of the authors and do not reflect the official policy or position of IQM.

[1] L. Viola and S. Lloyd, Phys. Rev. A **58**, 2733 (1998).
[2] L. Viola, E. Knill, and S. Lloyd, Phys. Rev. Lett. **82**, 2417 (1999).
[3] L. Viola and E. Knill, Phys. Rev. Lett. **94**, 060502 (2005).
[4] K. Khodjasteh and D. A. Lidar, Phys. Rev. Lett. **95**, 180501 (2005).
[5] K. Khodjasteh and D. A. Lidar, Phys. Rev. A **75**, 062310 (2007).
[6] D. Lidar, Adv. Chem. Phys. **154**, 295 (2012).
[7] W. Yang, Z.-Y. Wang, and R.-B. Liu, Front. Phys. **6**, 2 (2011).
[8] D. Suter and G. A. Álvarez, Rev. Mod. Phys. **88**, 041001 (2016).
[9] G. A. Álvarez, A. Ajoy, X. Peng, and D. Suter, Phys. Rev. A **82**, 042306 (2010).
[10] X. Peng, D. Suter, and D. A. Lidar, J. Phys. B: At. Mol. Opt. Phys. **44**, 154003 (2011).
[11] N. Ezzell, B. Pokharel, L. Tewala, G. Quiroz, and D. A. Lidar, Phys. Rev. Appl. **20**, 064027 (2023).
[12] B. Pokharel and D. A. Lidar, npj Quantum Inf. **10**, 23 (2024).
[13] P. Barthel, P. H. Huber, J. Casanova, I. Arrazola, D. Niroomand, T. Sriarunothai, M. B. Plenio, and C. Wunderlich, New J. Phys. **25**, 063023 (2023).
[14] W. Xu, T. Zhou, and K. e. a. Zhang, Phys. Rev. A **112**, 022435 (2025).
[15] C. Tong, H. Zhang, and B. Pokharel, PRX Quantum **6**, 030319 (2025).
[16] H. Y. Carr and E. M. Purcell, Phys. Rev. **94**, 630 (1954).
[17] S. Meiboom and D. Gill, Rev. Sci. Instrum. **29**, 688 (1958).
[18] G. S. Uhrig, Phys. Rev. Lett. **98**, 100504 (2007).
[19] A. M. Souza, G. A. Álvarez, and D. Suter, Philos. Trans. R. Soc. A **370**, 4748 (2012).
[20] A. A. Maudsley, J. Magn. Reson. **69**, 488 (1986).
[21] K. Khodjasteh and D. A. Lidar, Phys. Rev. Lett. **95**, 180501 (2005).
[22] J. R. West, B. H. Fong, and D. A. Lidar, Phys. Rev. Lett. **104**, 130501 (2010).
[23] M. A. Bernstein, K. F. King, and X. J. Zhou, *Handbook of MRI Pulse Sequences* (Elsevier, Amsterdam, 2004).
[24] G. T. Genov, D. Schraft, N. V. Vitanov, and T. Halfmann, Phys. Rev. Lett. **118**, 133202 (2017).
[25] D. G. Almeida, New fractional gates reduce circuit depth for utility-scale workloads (2024), accessed: 2025-08-12.
[26] IQM Quantum Computers, How IQM's pulse-level access is fuelling value for end-users (2025), accessed: 2025-09-08.